

connected to a frame grabbing board (Scion LG3) in a Macintosh computer. Frames were acquired at ~30 ms/frame and analyzed with NIH-Image.

30. D. Smetters, A. Majewska, R. Yuste, *Methods* **18**, 215 (1999).

31. L. C. Katz, A. Burkhalter, W. J. Dreyer, *Nature* **310**, 498 (1984).

32. Injections of fluorescent latex microspheres (Lu-mafluor) were made into the superior colliculus, 2 to 4 days before the experiment. Injection coordinates were tailored to the age.

33. We report SD in all measurements.

34. Every trigger-follower pair was recorded with biocytin-filled electrodes to recover morphologies following standard procedures (26). Neurons were reconstructed with a $\times 40/1.00$ NA objective, and contacts were identified with a $\times 100/1.3$ NA objective.

35. Supplementary information is available at www.sciencemag.org/cgi/content/full/293/5531/868/DC1.

36. To maximize followers' detection, we used ACSF containing 126 mM NaCl, 3 mM KCl, 26 mM NaHCO₃, 1 mM NaH₂PO₄, 2 mM CaCl₂, 1 to 2 mM MgSO₄, 10 mM dextrose, 5 μ M nicotine, 0.5 μ M 4-aminopyridine (4AP), and 0.5 μ M bicuculline. Followers can also be detected with normal or Mg-free ACSF (26). Experiments were done at 27°C. One to four followers were observed per trigger neuron, and followers chosen for dual recordings were reliably detected optically in $70 \pm 38\%$ of subsequent trials. Whole-cell recordings were performed with 6 to 9 megaohm pipettes, filled with 130 mM K-methylsulfonate, 11 mM biocytin, 10 mM KCl, 10 mM HEPES, 5 mM NaCl, 2.5 mM Mg-adenosine triphosphate, 0.3 mM Na-guanosine triphosphate, and 0 to 0.05 mM fura-2 pentapotassium salt (Molecular Probes). Dual recordings were made with an Axopatch 200B (Axon Instruments) and a BVC-700 (Dagan Instruments) amplifier and digitized with an A/D board (Instrutech) with Igor (Wavemetrics). For optical probing, a stereotyped spike train was used (10 pulses adapting over 200 ms, blue in Fig. 1D).

37. For each pixel, we defined the fluorescence change over time as $\Delta F/F = (F_1 - F_0)/F_0$, expressed in %, where F_1 is fluorescence at any time point and F_0 is fluorescence at the beginning of each trial. We tailored the imaging and analysis protocols to the kinetics of somatic calcium signals. To detect followers online, we computed a $\Delta F/F$ movie and adjusted the look-up table so that pixels recording calcium increases appeared light over a black background (Fig. 1D).

38. G. A. Marcoulides, S. L. Hershberger, *Multivariate Statistical Methods* (Lawrence Erlbaum Associates, Mahwah, NJ, 1997).

39. For each reconstructed neuron, we measured 18 morphological variables describing soma size and shape, dendrite number and total length, circular distribution of dendrites (vector averages), size and shape of the dendritic arborization (tile), distribution of dendrites along the radial axis, and depth of axonal ramification (Web table 1) (35). The positional data were not included in the cluster analysis. From these variables, we extracted the five principal components for follower clustering (Fig. 2B; eigenvalues > 1.0 ; Statistica) that accounted for most of the observed variance (89%); only the 11 standardized variables that made up the significant principal coordinates (absolute value > 0.7) were used. For large interneuron clustering (Web fig. 2B) (35), all variables were included and weighted as described below (44). Cluster analyses were performed with Ward's method (Statistica) and squared Euclidian distances.

40. Spike half-widths were averaged across at least 10 spikes in each cell, and means were averaged across cells in a class.

41. To measure facilitation and depression, we averaged responses to pairs of spikes (80-ms interval) over at least 10 trials and computed the mean changes in averaged EPSP peak amplitudes across cells in a class. In some instances, three to four spikes were presented at 80-ms intervals.

42. Responses in all interneurons were blindly classified as LTS or FS on the basis of standard criteria (M. Beierlein, personal communication).

43. For random sampling of interneurons, layer 5 neurons without apical dendrites were patched. Physiological re-

sponses to 800-ms current steps were examined to further confirm the nonpyramidal identity of recorded neurons.

44. To compare follower interneurons ($n = 10$) with the random sample ($n = 48$), we measured 19 variables from all cells. Our null hypothesis, that trigger axons contact interneurons randomly, was tested by comparing the original distribution of follower types with the density distribution of each randomly selected interneuron type in the neuropil. To achieve this, we weighted each randomly selected neuron on the basis of the length of its dendrites projected onto a plane, normalized to the cell with the longest dendrites. Weights were assigned on an integer scale from 1 to 10 (10 being the longest), and the MANOVA was significant both with and without a single outlier whose dendritic lengths exceeded the mean by 4 SD (upper left cell in Web fig. 2A) (35); all remaining weighted neurons' dendritic lengths were within 2 SD of the mean.

45. A. Swan, M. Sandilands, P. McCabe, *Introduction to Geological Data Analysis* (Blackwell Sciences, Oxford, 1995).

46. To correlate the axonal and dendritic arborizations, we constructed pairs of normalized probability density contour plots, using a 40- μ m region surrounding each process, and calculated the linear correlation between plots (Matlab).

47. A. Fairen, J. DeFelipe, J. Regidor, in *Cerebral Cortex*, vol. 1, A. Peters, E. G. Jones, Eds. (Plenum, New York, 1984), pp. 201–255.

48. J. S. Lund, *Annu. Rev. Neurosci.* **11**, 253 (1988).

49. We thank S. Giboni, Z. Peterlin, G. Tamas, and A. Tsiola for help and members of the laboratory for comments. This work was funded by the National Eye Institute, the National Institute of Mental Health, and the National Institute of Neurological Disorders and Stroke.

20 March 2001; accepted 12 June 2001

Sorting of Striatal and Cortical Interneurons Regulated by Semaphorin-Neuropilin Interactions

Oscar Marín,¹ Avraham Yaron,² Anil Bagri,² Marc Tessier-Lavigne,² John L. R. Rubenstein^{1*}

Most striatal and cortical interneurons arise from the basal telencephalon, later segregating to their respective targets. Here, we show that migrating cortical interneurons avoid entering the striatum because of a chemorepulsive signal composed at least in part of semaphorin 3A and semaphorin 3F. Migrating interneurons expressing neuropilins, receptors for semaphorins, are directed to the cortex; those lacking them go to the striatum. Loss of neuropilin function increases the number of interneurons that migrate into the striatum. These observations reveal a mechanism by which neuropilins mediate sorting of distinct neuronal populations into different brain structures, and provide evidence that, in addition to guiding axons, these receptors also control neuronal migration in the central nervous system.

Most striatal and cortical interneurons derive from a distant region in the basal telencephalon, the medial ganglionic eminence (MGE) (1–3). During development, interneurons migrate tangentially along stereotypical pathways to reach the striatum and the cortex, but the mechanisms that regulate their segregation into these two telencephalic subdivisions are not known.

To study the tangential migration of telencephalic interneurons, we used slice cultures (4) and transplanted portions of the MGE from green fluorescent protein (GFP)-expressing transgenic mice (5) into host slices obtained

from wild-type littermate embryos (Fig. 1). In agreement with previous reports (1–4), this assay consistently labeled a large number of migrating neurons whose transmission is mediated by γ -aminobutyric acid (GABA) (6). GFP-expressing cells followed two major routes in the basal telencephalon. Early migrations occurred superficial to the striatum [embryonic day 12 (E12); Fig. 1, A to D] (7), whereas later migrations (E13.5 and older) occurred primarily deep to the striatum (Fig. 1, E to H). Cells migrating toward the cortex seemed to avoid the striatum (Fig. 1, A to H), raising the possibility that cortical interneurons might be instructed to avoid the striatum to promote their migration into cortical territories. To test this hypothesis, we transplanted striatal tissue into the cortex (Fig. 1I). GFP-expressing cells migrating from the MGE avoided the ectopic striatum (Fig. 1, J and K), but migrated normally when a piece of piriform cortex was transplanted into the same location (Fig. 1, K to M).

¹Department of Psychiatry, Nina Ireland Laboratory of Developmental Neurobiology, Langley Porter Psychiatric Institute, ²Department of Anatomy, Howard Hughes Medical Institute (HHMI), and Department of Biochemistry and Biophysics, University of California, San Francisco, CA 94143, USA.

*To whom correspondence should be addressed. E-mail: jlrr@cgl.ucsf.edu

REPORTS

These results suggest that an extracellular signal present in the developing striatum repels cells migrating to the cortex.

Class 3 semaphorin proteins are chemorepellents for growing axons (8, 9), allowing them to avoid specific regions and channeling them into appropriate locations in fiber tracts (10). The similarity of this mechanism to our previous observations prompted us to investigate the role of semaphorins in directing interneuron migrations. We found that during the period of interneuron migration (E12 to E16), semaphorins 3A and 3F (Sema3A and Sema3F) are expressed in the striatum but are excluded from regions surrounding it (Fig. 2, A, B, E, and F). We next examined the expression of the high-affinity semaphorin receptors neuropilin1 and neuropilin2, which are required for mediating the repulsive effect of class 3 semaphorins on axons (8, 9). During the period of interneuron migration, neuropilin1 and neuropilin2 are expressed in the basal telencephalon in a pattern complementary to that of Sema3A and Sema3F—that is, in cells located either superficial or deep to the striatum but excluded from striatal cells (Fig. 2, C, D, H, and I). Comparison of this pattern with the pathways followed by migrating interneurons suggested that migrating cells might express these receptors. To test this hypothesis, we examined the expression of neuropilin1 and neuropilin2 in GFP-expressing cells or in cells containing GABA or calbindin (4). The distribution of neuropilin1 was analyzed using affinity-purified antibodies. To determine the distribution of cells expressing neuropilin2, we took advantage of the expression of β -galactosidase from the neuropilin2 locus in mice with a targeted mutation for this gene (11, 12). We found that neuropilin1 and neuropilin2 are expressed in many interneurons migrating into cortical territories (Fig. 2, G and J), but never in cells that invaded the striatum (6).

To confirm that neuropilin1 and neuropilin2 receptors are expressed in migrating interneurons, we studied *Dlx1/2* double mutants. In these mutants, interneurons fail to differentiate properly and accumulate in the subventricular zone (SVZ) of the basal telencephalon (3, 13). We found that many of these cells express high levels of neuropilin1 and neuropilin2 (6, 12). Ectopic neuropilin2-positive cells accumulated in periventricular ectopias within the SVZ. Some of these ectopias expressed neuropeptide Y (NPY) but did not express neuropilin1 (6, 12), suggesting that at least a large subpopulation of NPY interneurons exclusively express neuropilin2.

The pattern of expression of semaphorin proteins and their neuropilin receptors is consistent with a model in which cortical interneurons express neuropilin1 and/or neuropilin2 while migrating to the cortex and are repelled by striatal cells expressing Sema3A and Sema3F. To test this model, we placed aggregates of semaphorin-expressing COS cells (Sema3A,

Sema3F, or both) (11, 12) at the corticostriatal boundary in slice cultures and studied the migration of 1,1'-diiodoacetyl-3,3,3',3'-tetramethylindocarbocyanine perchlorate (DII)-labeled cells from the MGE (Fig. 3A). As a control, aggregates of GFP-expressing COS cells were placed on the opposite side of the slices (Fig. 3A). Cell aggregates expressing both Sema3A and Sema3F blocked the migration of interneurons into the dorsal cortex (Fig. 3, B to D, F, and G). In contrast, cell aggregates expressing exclusively Sema3A (which operates via neuropilin1 receptors) or Sema3F (which operates via neuropilin2 receptors) (8, 9) only partially arrested the migration of cortical interneurons (Fig. 3, E and G). Moreover, whereas migrating cells orient what appears to be

their leading process toward the cortex when they approach the control aggregates (Fig. 3, H and J), most cells that approached the Sema3A/3F-expressing aggregates turn their processes away from them (Fig. 3, I and J).

We next performed loss-of-function experiments, first analyzing the migration of telencephalic interneurons in neuropilin2 mutants (11). To avoid the possible redundant functions of neuropilin1 and neuropilin2 in tangential migrations at later embryonic stages, we analyzed the pattern of tangential migration in slices derived from E12 brains. At this age, neuropilin2, but not neuropilin1, is expressed in cells tangentially migrating into the piriform cortex (Fig. 2D), suggesting that loss of neuropilin2 function at this stage should not be compensated by neuro-

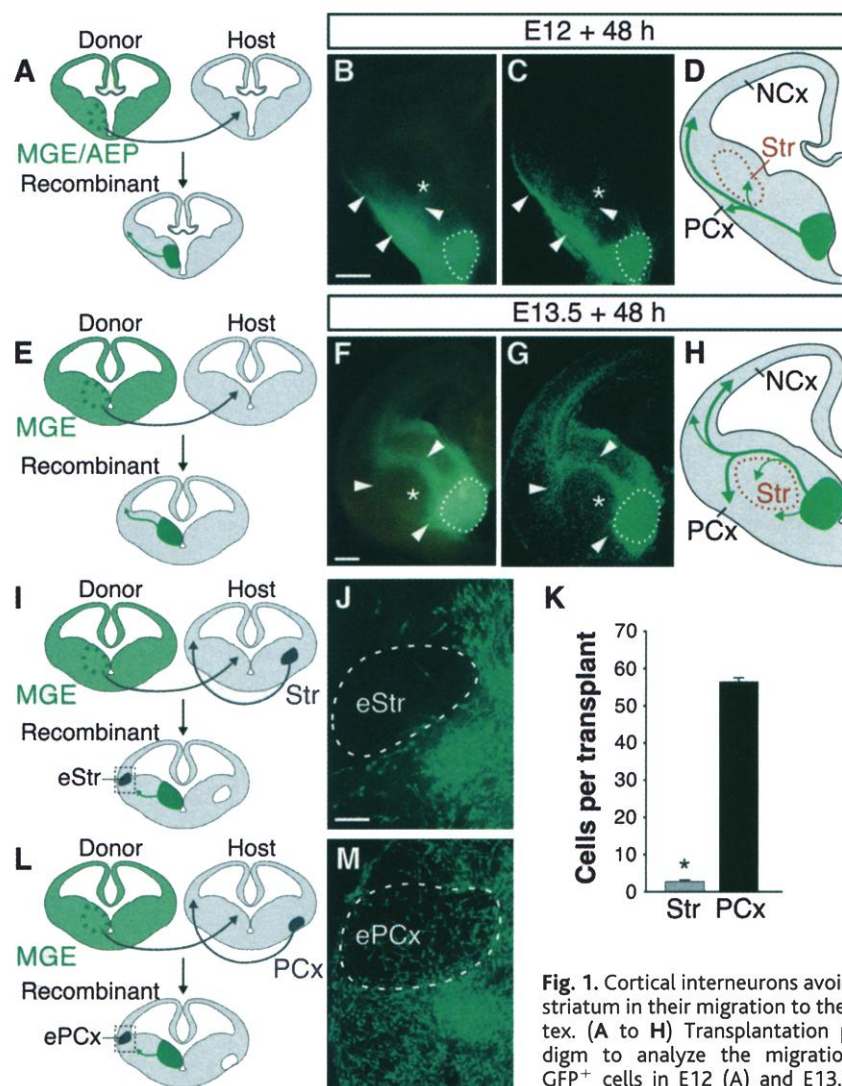


Fig. 1. Cortical interneurons avoid the striatum in their migration to the cortex. (A to H) Transplantation paradigm to analyze the migration of GFP⁺ cells in E12 (A) and E13.5 (E) living coronal slices (B and F) or after immunohistochemistry against GFP (C and G). Arrowheads, migrating cells; asterisks, striatum (Str); dotted outlines, grafts. Scale bars, 200 μ m. Schematic representations of cell migration routes are shown for E12 (D) and E13.5 (H). AEP, anterior entopeduncular region; MGE, medial ganglionic eminence; NCx, neocortex; PCx, piriform cortex. (I to M) Transplantation paradigm to analyze the migration of cortical interneurons into an ectopic striatum (eStr) (I) or piriform cortex (ePCx) (L). Dashed lines in (J) and (M), ectopic tissue; scale bar, 100 μ m. Numbers of cells migrating into ectopic tissue ($n = 12$) are quantified in (K); histograms show averages \pm SE. χ^2 test, * $P < 0.0001$.

REPORTS

pilin1 signaling. For this set of experiments, we adapted an electroporation method to transfect a *Gfp* expression vector into the MGE in slice cultures (Fig. 4A) (12). In control experiments, most GFP-expressing cells migrated superficial

to the striatum on their way to the cortex (Fig. 4, B and C). In contrast, in slices from neuropilin2 mutants, most GFP-expressing cells migrated directly into the striatum (Fig. 4, D and E). These results suggest that loss of neuropilin2

signaling may result in an imbalance in the number of interneurons in the striatum or cortex. Consistent with this, the developing striatum of neuropilin2 mutants contained numerous ectopic neuropilin2-expressing cells, identified by ex-

Fig. 2. Complementary expression of class 3 semaphorins and their receptors in the developing telencephalon during the period of interneuron migration. (A to F, H and I) Serial coronal sections through the telencephalon showing *Sema3A* (A and E) and *Sema3F* (B and F) expression in the striatum, and *neuropilin1* (C and H) and *neuropilin2* (D and I) expression in adjacent regions. Open and solid arrowheads in (D), (H), and (I) point to superficial and deep migrations, respectively. (G) GFP (green) and neuropilin1 (red) colocalization in an MGE-derived cell migrating into the cortex (solid arrowheads). Other neuropilin1⁺ cells are not labeled with GFP (open arrowheads). (J) β -galactosidase (green puncta, arrowheads) and calbindin (red) colocalization in a cell migrating into the cortex. Dotted squares in (H) and (I) show the location of the cells shown in (G) and (J), respectively. Scale bars, 200 μ m (A to D), 100 μ m (E, F, H, and I), 10 μ m (G and J).

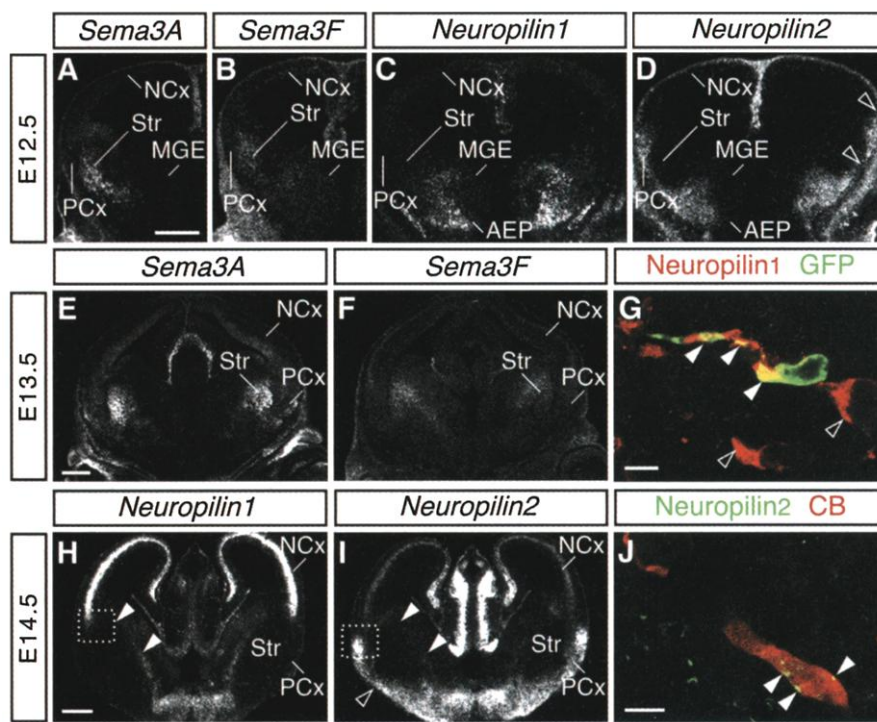
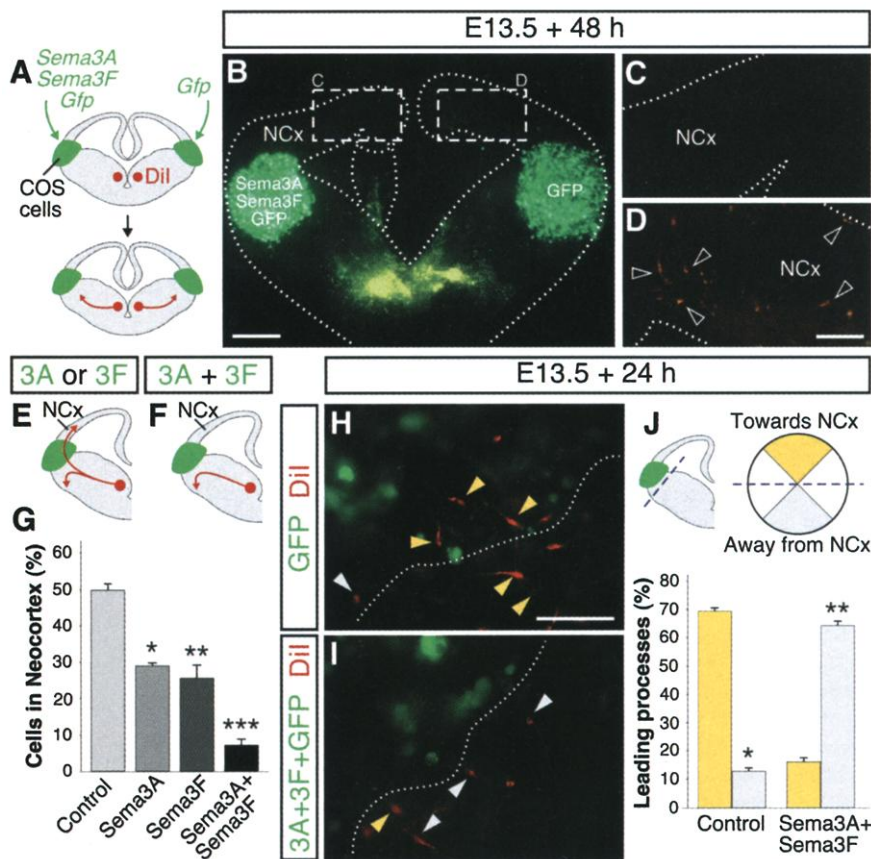


Fig. 3. Ectopic expression of *Sema3A* and *Sema3F* blocks the migration of cortical interneurons. (A) Experimental paradigm. (B) Coronal slice through the telencephalon. (C and D) Higher magnification of the experimental (C) and control cortex (D). Arrowheads, Dil-labeled cells. Dotted lines, slice outline. (E and F) Schematic diagrams illustrating the results obtained in experiments where COS cells were transfected with either *Sema3A* or *Sema3F* (E) or both simultaneously (F). (G) Quantification of the effect of semaphorin-expressing cells on the migration of MGE-derived cells ($n > 20$). χ^2 test, * $P < 0.001$, ** $P < 0.001$, *** $P < 0.0001$. (H and I) Migrating cells penetrate through control COS cells (H) but are repelled by cells expressing semaphorins (I). Yellow and gray arrowheads point to cells migrating toward or away from the cortex, respectively. Dotted lines, cell aggregate outline. (J) Quantification of the effect of semaphorin-expressing cells on the orientation of leading processes ($n = 20$). χ^2 test, * $P < 0.0001$, ** $P < 0.0001$. Scale bars, 400 μ m (B), 100 μ m (C, D, H, and I).



pression of β -galactosidase from the neuropilin2 locus (Fig. 4, F and G) (12), and adult mice lacking neuropilin2 had about twice as many striatal NPY-expressing interneurons as did controls (Fig. 4, H to J) (12, 14). Thus, neuropilin2 appears to be required in vivo for sorting of migrating cortical and striatal interneurons to their correct destination.

Neuropilin1 mutant mice die by E13.5 (15), precluding the analysis of interneuron migration in these animals. To circumvent this problem, we expressed a dominant-negative form of neuropilin1 (Nrp1dn) in migrating neurons (12, 16). Coelectroporation of *Gfp* and *Nrp1dn* (17) into the MGE in slice cultures resulted in a drastic reduction in the number of neurons migrating into the cortex (Fig. 4, K to O) (12, 18). To eliminate the possibility that expression of Nrp1dn simply prevents the normal migration of MGE-derived cells, we coelectroporated *Gfp* and *Nrp1dn* into the MGE and cultured it in matrigel (BD Biosciences). Migration of GFP/Nrp1dn-expressing cells (17) was indistinguishable from that observed in cells electroporated with *Gfp* alone (12), suggesting that expression

of Nrp1dn does not nonspecifically impair cell migration. Thus, signaling through neuropilin1 receptors appears also to be required for proper segregation of cortical and striatal interneurons.

Our results indicate that neuropilin receptors are required for the sorting of striatal and cortical interneurons. MGE-derived interneurons directed toward the cortex express semaphorin receptors (neuropilin1, neuropilin2, or both) as they migrate. Striatal cells express *Sema3A* and *Sema3F*, which presumably contribute to creating an exclusion zone for interneurons migrating to the cortex, channeling them into adjacent paths. In the absence of loss-of-function data for *Sema3A* and *Sema3F*, we cannot exclude the possibility that additional neuropilin ligands expressed in the striatum also contribute to this repulsive activity. Finally, MGE-derived interneurons migrating into the striatum either never express neuropilins or down-regulate their expression before entering the striatum. We suggest that the final destination of tangentially migrating interneurons (striatum or cortex) is determined by expression of neuropilin1 and neuropilin2.

Our results implicate neuropilin receptors and their semaphorin ligands in the control of neuronal migration in the central nervous system (CNS), a role previously proposed for other axon guidance systems, such as the netrin-1/DCC and Slit/Robo (19) systems. In vitro experiments suggest that *Sema3A* may also pattern chick neural crest migration (20). We suggest that neuropilins and semaphorins sort and channel different populations of migratory neurons into distinct paths. The creation of selective exclusion zones for subpopulations of migrating neurons may represent a general role for neuropilins and semaphorins in the formation of functional boundaries between different neuronal populations during development of the CNS.

References and Notes

1. S. Anderson, M. Mione, K. Yun, J. L. Rubenstein, *Cereb. Cortex* **9**, 646 (1999).
2. J. C. Parnavelas, *Trends Neurosci.* **23**, 126 (2000).
3. O. Marín, S. A. Anderson, J. L. R. Rubenstein, *J. Neurosci.* **20**, 6063 (2000).
4. S. A. Anderson, O. Marín, C. Horn, K. Jennings, J. L. R. Rubenstein, *Development* **128**, 353 (2001).
5. A. K. Hadjantonakis, M. Gertsenstein, M. Ikawa, M. Okabe, A. Nagy, *Mech. Dev.* **76**, 79 (1998).
6. O. Marín, A. Yarom, A. Bagri, M. Tessier-Lavigne, J. L. R. Rubenstein, data not shown.
7. Regions ventral to the MGE (the anterior entopeduncular region and the preoptic area) also appear to contribute to this early and superficial migration to the cortex.
8. J. A. Raper, *Curr. Opin. Neurobiol.* **10**, 88 (2000).
9. L. Tamagnone, P. M. Comoglio, *Trends Cell Biol.* **10**, 377 (2000).
10. Y. Zou, E. Stoekli, H. Chen, M. Tessier-Lavigne, *Cell* **102**, 363 (2000).
11. H. Chen et al., *Neuron* **25**, 43 (2000).
12. Supplementary figures and details of experimental procedures are available at Science Online at www.sciencemag.org/cgi/content/full/293/5531/872/DC1.
13. S. A. Anderson et al., *Neuron* **19**, 27 (1997).
14. Approximately 30% of the cases (4 of 14).
15. T. Kawasaki et al., *Development* **126**, 4895 (1999).
16. M. J. Renzi, T. L. Wexler, J. A. Raper, *Neuron* **28**, 437 (2000).
17. Analysis of the expression of GFP and Nrp1dn in slice cultures ($n = 5$) demonstrates extensive (>95%) coelectroporation of both plasmids.
18. Numbers of labeled cells per cortex were 60.4 ± 2.9 (average \pm SE) in control slices, 12.9 ± 3.2 in GFP + Nrp1dn slices. χ^2 test, $P < 0.001$ ($n = 14$).
19. A. Chisholm, M. Tessier-Lavigne, *Curr. Opin. Neurobiol.* **9**, 603 (1999).
20. B. J. Eickholt, S. L. Mackenzie, A. Graham, F. S. Walsh, P. Doherty, *Development* **126**, 2181 (1999).
21. We thank J. Baker for assistance; S. Anderson and B. Rico for comments; T. Stühmer for help with electroporation; J. Miyazaki for pCAGGS vector (12); A. Kolodkin, A. Holtmaat, and J. Verhaagen for neuropilin1 antibodies; M. Sheng and Y.-P. Hsueh for TBR1 antibodies (12); and A. Nagy for GFP mice. We also thank N. Tamamaki for sharing results prior to publication and for coordinating the initial submission of papers from both laboratories. O.M. is a National Alliance for Research on Schizophrenia and Depression (NARSAD) Young Investigator Award recipient and a Medical Investigation of Neurodevelopmental Disorders (MIND) Institute Scholar. A.Y. is supported by a fellowship from the Human Frontier Science Program. A.B. is an Epilepsy Foundation of America predoctoral fellow. Supported by a grant from Nina Ireland Laboratory, National Institute on Drug Abuse grant R01DA12462, and National Institute of Mental Health grants R01MH49428-01, R01MH51561-01A1, and K02MH01046-01 (J.L.R.R.). M.T.-L. is an Investigator of the HHMI.

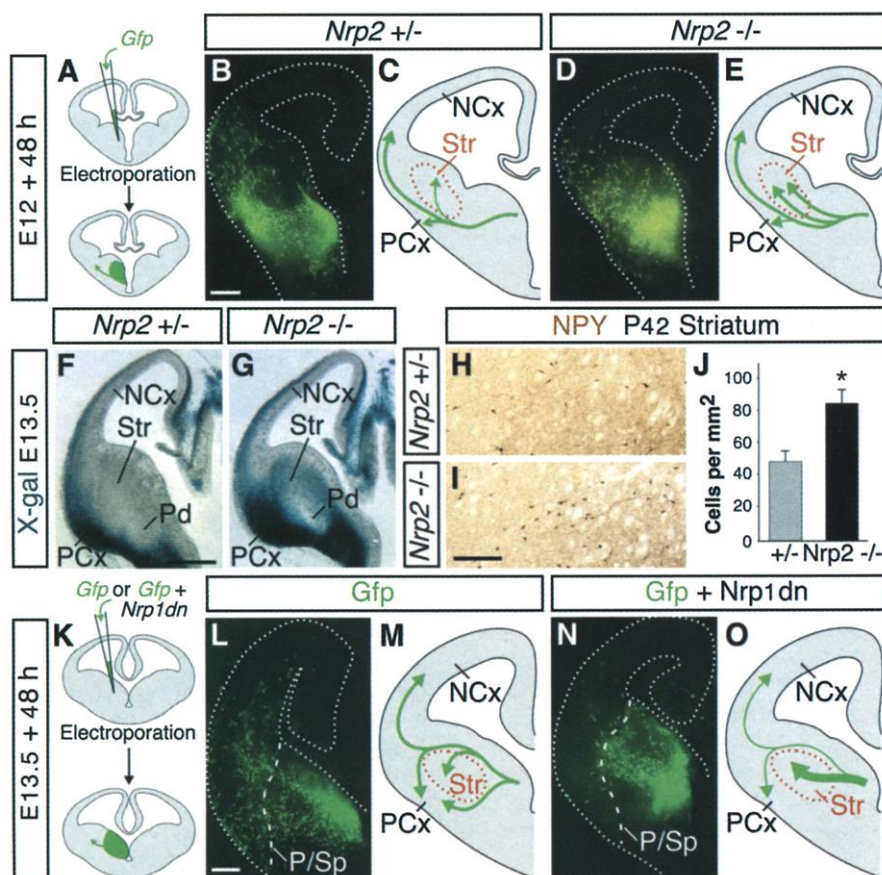


Fig. 4. Loss of neuropilin function perturbs the migration of cortical interneurons. (A) Experimental paradigm. (B and D) Migration of cells electroporated with a *Gfp* expression vector ($n = 8/8$). (C and E) Schematic representation of migratory routes. (F and G) X-Gal staining of coronal sections through the telencephalon ($n = 6/6$). (H and I) NPY immunohistochemistry. (J) Quantification of the number of NPY⁺ cells in the striatum of *Nrp2*^{+/-} and *Nrp2*^{-/-} mice. χ^2 test, $*P < 0.001$ ($n = 4$). (K) Experimental paradigm. (L and N) Migration of cells electroporated with a *Gfp* expression vector alone (L) or with *Gfp* and *Nrp1dn* expression vectors (N). (M and O) Schematic representation of migratory routes. Dotted lines, slice outline; P/Sp, pallial-subpallial boundary; Pd, pallidum. Scale bar, 200 μ m.

23 April 2001; accepted 3 July 2001